Using a Solution Crystal Growth Method To Grow Arrays of Aligned, Individually Distinct, Single-Crystalline TiO_2 Nanoneedles within Nanocavities

Chin-Cheng Weng,[†] Chen-Ping Chen,[†] Ching-Hua Ting,[‡] and Kung-Hwa Wei*[,†,‡]

Department of Materials Science and Engineering and Center for Nano Science and Technology, National Chiao Tung University, 1001 Ta Hsueh Road, Hsinchu, Taiwan 300, Republic of China

Received March 29, 2005
Revised Manuscript Received May 21, 2005

Titanium dioxide (TiO_2) is one of the most important semiconductor materials. It is used widely (a) in photovoltaic cells, photonic crystals, photocatalysis, ultraviolet blockers, and smart surface coatings, (b) for sensing, optical emission, and selective adsorption, and (c) as a functional filling material in textiles, paints, paper, and cosmetics.[1] In recent years, ordered and aligned TiO_2 nanostructures have been prepared using a number of templating techniques. For example, ordered TiO_2 nanotubes have been synthesized through sol−gel processing using porous anodic alumina as the template[2,3] and arrays of TiO_2 nanowires have been synthesized electrochemically.[4] We reported recently the synthesis of arrayed TiO_2 nanoneedles from ordered TiO_2 seeds that we had incorporated into one block of a thin layer of a PS-*b*-P4VP diblock copolymer.[5] To the best of our knowledge, the growth of individually distinct rods, which are important components in some applications, has yet to be described. In this communication, we report that single, aligned TiO_2 nanoneedles having diameters in the tens of nanometers can be grown through a crystal growth in solution process from patterned nanocavities under the influence of an electric field. The electric field, which we applied perpendicular to the substrate plane, drove the precursor solution into the cavities by overcoming the surface tension encountered and oriented the TiO_2 nanoneedles during the growth process. This method is a new and simple approach for the synthesis of arrays of individual and aligned TiO_2 nanoneedles.

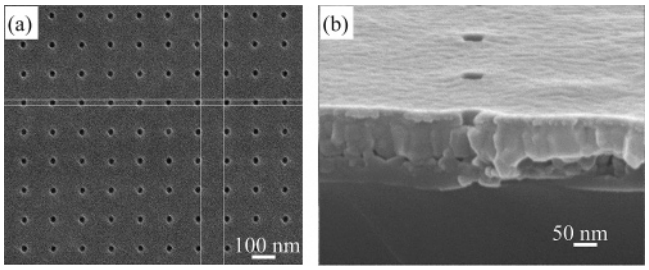

Figure 1. SEM images of a nanopatterned array of 50-nm cavities. (a) Plan view. (b) Cross-sectional image.

We deposited a thin layer (ca. 100 nm) of TiO_2 onto a Si wafer and then used E-beam lithography (JEOL JSM-6500F and DEBEN PCD BEAM BLANKER) to create holes of different sizes (30−100 nm) within a PMMA photoresist. We prepared the 50-nm photoresist layer (Micro Chem, 495 PMMA A3) by spin-coating on the TiO_2 layer of the Si wafer. After the E-beam writing, we used methyl isobutyl ketone/IPA to develop (25 °C, 70 s) the nanopatterned arrays of 30−100-nm cavities. Figures 1a and 1b display the in-plane and cross-sectional images, respectively, of 50-nm holes. We prepared precursor solutions having Ti concentrations over the range from 0.1 mM to 0.1 M by adding $TiOSO_4 \cdot xH_2O$ at room temperature into aqueous solutions of hydrochloric acid (HCl) containing urea; the molar ratios (R) of urea to Ti were between 100 and 500. After stirring for 1 h, we adjusted the initial value of the pH (pH_i) of each solution to 1.0, 1.2, or 1.4. We chose $TiOSO_4$ as the starting material because of its low cost, low reactivity with moisture, and lack of toxicity.[5,6] The substrates were immersed in the precursor solutions maintained at 95 °C. After a reaction time of 6 h, the substrates deposited with TiO_2 were washed with acetone under weak ultrasonic stimulation to remove the photoresist, rinsed with deionized water, and then dried at room temperature. The applied electric field was controlled up to 750 V/cm. Scheme 1a displays the processes for synthesizing aligned single TiO_2 nanoneedles and growing the nuclei confined within the holes; Scheme 1b indicates how a limited number of nuclei may reside in a nanocavity and grow to form a single particle.

Figure 2 displays the arrays of TiO_2 nanoneedles that we prepared using different cavity sizes; the arrays were grown while applying an electric field of 625 V/cm. After a reaction time of 6 h, we observed that flowerlike TiO_2 particles, which consist of a few TiO_2 nanoneedles, formed on the substrate surface patterned with 100-nm-sized nanocavities (Figure 2a). When we decreased the sizes of the holes to 50 nm, the number of branches of the TiO_2 flowers decreased (Figure 2b). When each nanocavity's size was 30 nm (Figure 2c),

* To whom correspondence should be addressed. Tel: 886-35-731871. Fax: 886-35-724727. E-mail: khwei@cc.nctu.edu.tw.
† Department of Materials Science and Engineering.
‡ Center for Nano Science and Technology.

(1) (a) O'Regan B. C.; Lenzmann F. *J. Phys. Chem. B* **2004,** *108*, 4342. (b) Jeon S.; Braun, P. V. *Chem. Mater.* **2003,** *15*, 1256. (c) Adachi, M.; Okada, I.; Ngamsinlapasathian, S.; Murata, Y.; Yoshikawa, S. *Electrochemistry* **2002**, *70*, 449. (d) Li, D.; Xia, Y. N. *Nano Lett.* **2003**, *3*, 555.
(2) Hulteen, J. C.; Martin, C. R. *J. Mater. Chem.* **1997**, *7*, 1075.
(3) (a) Hoyer, P. *Langmuir* **1996**, *12*, 1411. (b) Lakshmi, B. B.; Dorhout, P. K.; Martin, C. R. *Chem. Mater.* **1997**, *9*, 857. (c) Lakshmi, B. B.; Patrissi, C. J.; Martin, C. R. *Chem. Mater.* **1997**, *9*, 2544. (d) Zhang, X. Y.; Zhang, L. D.; Chen, W.; Meng, G. W.; Zheng, M. J.; Zhao, L. X. *Chem. Mater.* **2001**, *13*, 2511. (e) Liu, S. M.; Gan, L. M.; Liu, L. H.; Zhang, W. D.; Zeng, H. C. *Chem. Mater.* **2002**, *14*, 1391. (f) Lei, Y.; Zhang, L. D.; Meng, G. W.; Li, G. H.; Zhang, X. Y.; Liang, C. H.; Cheng, W.; Wang, S. X. *Appl. Phys. Lett.* **2001**, *78*, 1125.
(4) Miao, Z.; Xu, D.; Ouyang, J.; Guo, G.; Zhao, X.; Tang, Y. *Nano Lett.* **2002**, *2*, 717.
(5) (a) Weng, C. C.; Wei, K. H. *Chem. Mater.* **2003**, *15*, 2936. (b) Weng, C. C.; Hsu, K. F.; Wei, K. H. *Chem. Mater.* **2004**, *16*, 4080.
(6) (a) Yamabi, S.; Imai, H. *Chem. Mater.* **2002**, *14*, 609. (b) Yamabi, S.; Imai, H. *Chem. Lett.* **2001**, *30*, 220. (c) Sathyamoorthy, S.; Moggridge, G. D.; Hounslow, M. J. *Cryst. Growth Des.* **2001**, *1*, 123. (d) Yang, H. G.; Zeng, H. C. *J. Phys. Chem. B* **2003**, *107*, 12244. (e) Kandori, K.; Kon-no, K.; Kitahara, A. *J. Colloid Interface Sci.* **1988**, *122*, 78.

10.1021/cm0506712 CCC: $30.25
Published on Web 06/04/2005

Scheme 1. Graphical Representations of (a) the Synthesis of Aligned Single TiO_2 Nanoneedles and (b) the Growth of Nuclei within Nanocavities

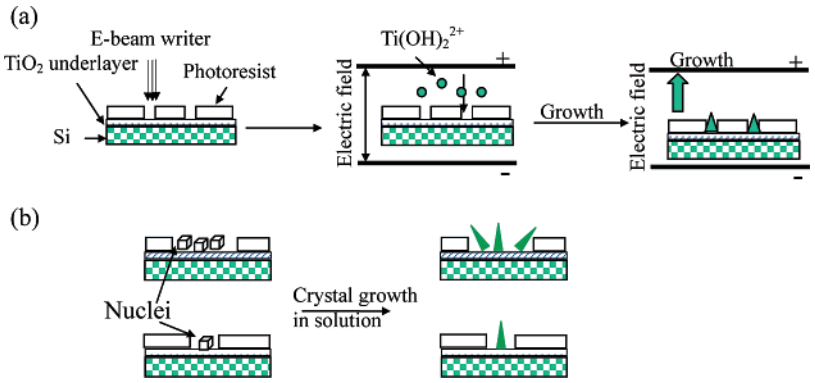

most of the TiO_2 particles that grew on the substrate were single nanoneedles (i.e., without branches) and, additionally, they were aligned; Figure 2d presents a scanning electron microscopy image of the tilted substrate. This result suggests that the size of the cavity determines the degree of branching of the TiO_2 nanoneedles that grow from a single cavity. No TiO_2 nanoneedles grew in nanocavities smaller than 50 nm unless an electric field was present. In the case of the 30-nm cavities, we grew the single and aligned TiO_2 nanoneedles, which can be either rutile or anatase depending on the pH value of the solution, under an applied field of 625 V/cm.

Figure 3 displays a high-resolution transmission electron microscopy (HRTEM) image of a typical TiO_2 nanoneedle obtained after reacting the mixture at 95 °C for 6 h and using a 5×10^{-4} M Ti precursor aqueous solution (pH_i 1.0; $R =$ 200). The TiO_2 nanoneedle is greater than 80-nm long and 30-nm wide and possesses a sharp pinnacle at its tip. In the inset of Figure 3a, the spacing between adjacent lattice planes of a simple TiO_2 needle is ca. 3.2 Å, which corresponds to the distance between the (110) crystal planes of the rutile phase. Figure 3b displays a selected area electron diffraction (SAED) pattern. Three typical diffraction spots are indexed to the 111, 110, and 220 planes by considering their ratios of $1/\boldsymbol{d}_{hkl}$.

Figure 4 presents plan-view SEM images (15° tilted) of TiO_2 nanoneedle arrays grown at pH_i 1.4 from nanocavities having sizes of (a) 100, (b) 50, and (c) 30 nm. At this higher pH_i, we observe that wider TiO_2 plates formed and grew into multiplate nanoneedles. Even when the size of the confining holes decreased to 30 nm, on this substrate we did not observe any single, aligned TiO_2 nanoneedles that resemble those presented in Figure 2c. Moreover, most of the plates formed at pH_i 1.4 are larger than the original cavity size and the lengths of nanoneedles are obviously shorter than those of the TiO_2 particles grown at pH_i 1.0.

Although the shape and crystal phase of the TiO_2 nanoneedles can be controlled by changing the values of the pH_i,

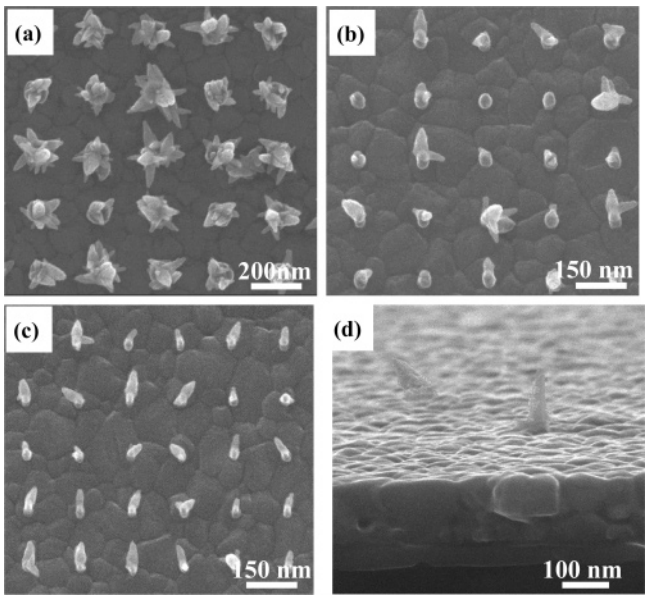

Figure 2. SEM images (plan views, tilted 15°) of arrays of TiO_2 nanoneedles grown from nanocavities sized at (a) 100, (b) 50, and (c) 30 nm. The concentration of the Ti precursor solution was 5×10^{-4} M, the ratio R was 200, the value of the initial pH was 1.0, and the applied electric field was 625 V/cm. (d) Cross-sectional image of the TiO_2 nanoneedles grown from the 30-nm-sized nanocavities.

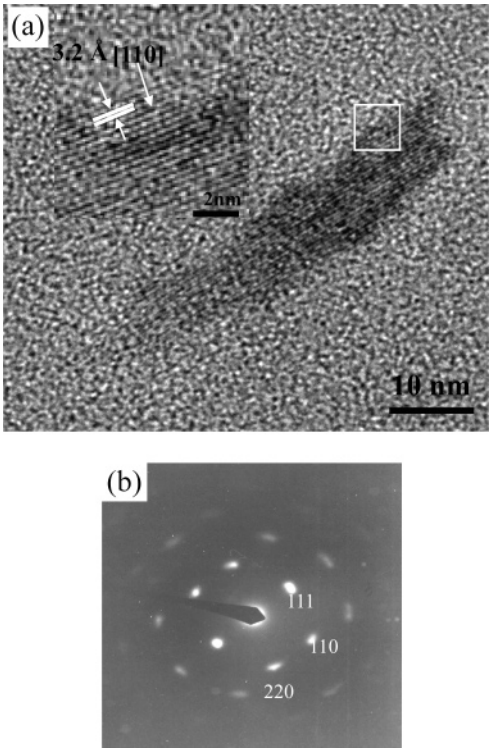

Figure 3. (a) An HRTEM image of a rutile TiO_2 nanoneedle. The spacing between adjacent (110) lattice planes is ca. 3.2 Å. (b) An SAED pattern indicating that the TiO_2 particle possesses a rutile crystal phase.

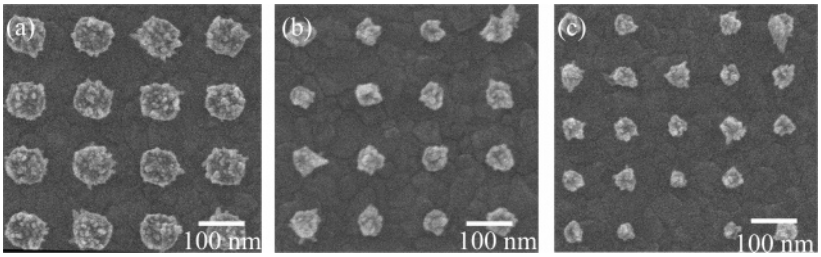

Figure 4. SEM images (plan views, tilted 15°) of arrays of TiO_2 nanoneedles grown from nanocavities sized at (a) 100, (b) 50, and (c) 30 nm. The concentration of the Ti precursor solution was 5×10^{-4} M, the ratio R was 200, the value of the initial pH was 1.4, and the applied electric field was 625 V/cm.

the ratio R, and the Ti precursor concentration,[7,8] the individually distinct single-crystalline TiO_2 nanoneedles formed only under a strict set of conditions. When we changed the value of pH_i from 1.0 to 1.4 and R was 200, the initial growth of TiO_2 was in the form of wide plates and multiple needles formed in the confining cavities. At a value of pH_i slightly higher than 1.0, the conditions in solution are closer to the thermodynamic equilibrium between $Ti(OH)_2^{2+}$/rutile or $Ti(OH)_2^{2+}$/anatase.[6a] This situation causes too many TiO_2 nuclei to form simultaneously within the cavities. Concurrently, the value of pH of the solution increases as the urea decomposes, which causes the nuclei to form rapidly. The TiO_2 underlayer in rutile phase facilitates the growth of vertical TiO_2 needles in the nanocavities across the photoresist layer homogeneously. Without this underlayer, the vertical growth of TiO_2 needles was more difficult. The effect of crystal phase of TiO_2 underlayer on the crystal phase of grown TiO_2 needles depends on the pH value of the solution. For instance, as the value of the pH_i increases to more than 1.4, the crystal phase of the grown TiO_2 nanoneedles changes from rutile to anatase.

It is well-known that the surfaces of rutile and anatase have different wettabilities that depend on the crystal plane.[9,10] The (00*l*) planes of rutile and anatase, which are perpendicular to the *c* axis, are comparatively inert in the absence of more reactive bridging site oxygen atoms. Other crystal planes that possess bridging site oxygen atoms and are parallel to the *c* axis are relatively hydrophilic. Crystal growth perpendicular to the *c* axis is suppressed when coexisting species, such as urea and ammonium ions, become adsorbed selectively onto the more hydrophilic surfaces that exist parallel to the *c* axis of the crystallites. This phenomenon results in the preferred growth toward needlelike TiO_2 structures, rather than disklike structures. For instance, Figure 5 shows that the orientation of an anatase TiO_2 needle is along the [002] direction with the spacing between adjacent lattice planes to be ca. 4.7 Å as determined by HRTEM/SAED experiments. On the other hand, increasing the molar ratio of urea to titanium should result in TiO_2 nanoneedles having higher aspect ratios. Indeed, when the ratio R is over 300, the value of the pH rises quickly because of decomposition of urea; this phenomenon leads to increased precipitation in the aqueous solution and a decrease in deposition because the aqueous solutions quickly become supersaturated with TiO_2. In our study, we found that the best conditions for obtaining long, single TiO_2 nanoneedles were a pH_i of 1.0−1.2 and a ratio R of 150−300.

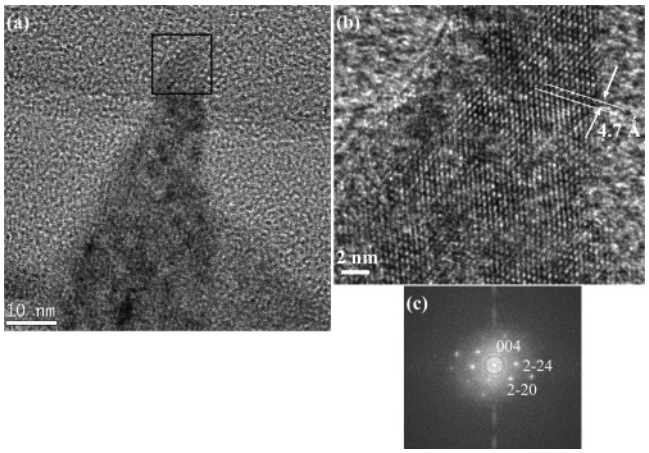

Figure 5. (a) An HRTEM image of an anatase TiO_2 needle. (b) The spacing between adjacent (002) lattice planes is ca. 4.7 Å as shown in the enlarged section. (c) An SAED pattern indicating that the TiO_2 needle possesses an anatase crystal phase.

In summary, we have fabricated arrays of single, aligned TiO_2 nanoneedles within nanocavities by using a solution crystal growth process under an applied electric field. The values of pH_i and the ratio R both affect the morphology of the TiO_2 nanoneedles. When the pH_i was >1.2, the nuclei formed too quickly and we did not fabricate any single needles; when the ratio R was larger than 300, needles did not form within the nanocavities. We believe that this new class of aligned TiO_2 nanostructures will find a wide range of future applications.

Acknowledgment. We appreciate the financial support provided by the National Science Council, Taiwan, through Project NSC 94-2120-M-009-001.

Supporting Information Available: Additional details (PDF). This material is available free of charge via the Internet at http://pubs.acs.org.

CM0506712

(7) Yamabi, S.; Imai, H. *Thin Solid Films* **2003,** *434*, 86.
(8) Goh, G. K. L.; Donthu, S. K.; Pallathadka, P. K. *Chem. Mater.* **2004**, *16*, 2857.
(9) (a) Oskam, G.; Nellore, A.; Penn, R. L.; Searson, P. C. *J. Phys. Chem.* **2003**, *107*, 1734. (b) Wang, R.; Hashimoto, K.; Fujishima, A.; Chikuni, M.; Kojima, E.; Kitamura, A.; Shimohigoshi, M.; Watanabe, T. *Nature* **1997**, *388*, 431.
(10) (a) Wang, R.; Sakai, N.; Fujishima, A.; Watanabe, T.; Hashimoto, K. *J. Phys. Chem. B* **1999**, *103*, 2188. (b) Watanabe, T.; Nakajima, A.; Wang, R.; Minabe, M.; Koizumi, S.; Fujishima, A.; Hashimoto, K. *Thin Solid Films* **1999**, *351*, 260.